Topology of forward scattering of neutrons from imperfect multilayers

G. P. Felcher and R. J. Goyette
Argonne National Laboratory, Argonne, Illinois 60439

S. Anastasiadis* and T. P. Russell
IBM Almaden Research Center, San Jose, California 95120

M. Foster† and F. Bates
Department of Chemical Engineering, University of Minnesota, Minneapolis, Minnesota 55455
(Received 6 May 1994)

Neutrons sent at grazing incidence on imperfect multilayers of polymers are scattered both out of and within the plane of reflection. In the latter geometry the scattered intensity is highly structured in two series of ridges, whose loci can be labeled in terms of the neutron momenta. Intersecting ridges show evidence of mode coupling. Similar topology is expected for x-ray scattering.

Small-angle-scattering experiments of neutrons or x rays are routinely used to determine the size, shape, and spatial organization of "particles" dispersed in a medium. The scattering entities may be macromolecules or micelles in a solvent or pores or precipitates in a solid, with sizes ranging from 10 to 1000 Å. Small-angle scattering is conventionally performed in transmission geometry[1] and the scattered intensity is measured starting with angles as close to the incident beam as possible. The recorded intensity versus angle is translated, with the help of standards,[2] into an absolute differential scattering cross section as a function of the momentum transferred, $q=4\pi\sin\theta/\lambda$, where λ is the wavelength of the incident radiation and θ the angle of scattering. If the scattering power of the particles comprised in the system is weak, only single scattering needs to be considered and the kinematic, or first Born approximation retains its validity.

Small-angle scattering may also be observed in grazing incidence geometry. In this configuration (Fig. 1) the incident beam is in part reflected from the surface, in part refracted through it. Layers parallel to the surface also partially reflect the beam, and from the intensity reflected as a function of $q_z=q$ (the component of the momentum transfer perpendicular to the sample surface), the depth profile of the material may be obtained to fine detail.[3,4] Planar imperfections (such as rough surfaces or interfaces, undulation of the layers, or lateral inhomogeneities within the layers) scatter neutron away from the reflected beam. The scattering may take place within the plane of reflection defined by the angle of incidence θ_i and reflection θ_f, or else at an angle $\Delta\phi$ *out* of the reflection plane. There is an important difference between the two cases, and to avoid confusion the scattering in the plane of reflection will be named "*forward* scattering." Dishomogeneities in the plane of the film may be represented by a reciprocal plane vector τ with components τ_x and τ_y, respectively, in the reflection plane and perpendicular to it (Fig. 1). When $|\tau|\ll q_z$ the conservation of energy and momentum for the scattered beam require that

$$\tau_x=|k|\sin\theta_i\Delta\theta\ ,\qquad \tau_y=|k|\Delta\phi\ , \tag{1}$$

where $|k|=2\pi/\lambda$ and $\Delta\theta$ is the angle between the scattered and the reflected beam in the reflection plane. If the lateral fluctuations are isotropic in the plane of the film ($\tau_x=\tau_y$) scattering might be present at a detectable $\Delta\theta$ even when $\Delta\phi$ is negligibly small. The expression for lateral scattering is identical to that for small-angle scattering in transmission geometry. Forward scattering is instead observable for particles on the micron size scale.[5,6] The question is, can the intensity scattered at grazing incidence be translated into a reliable density-density correlation in real space?

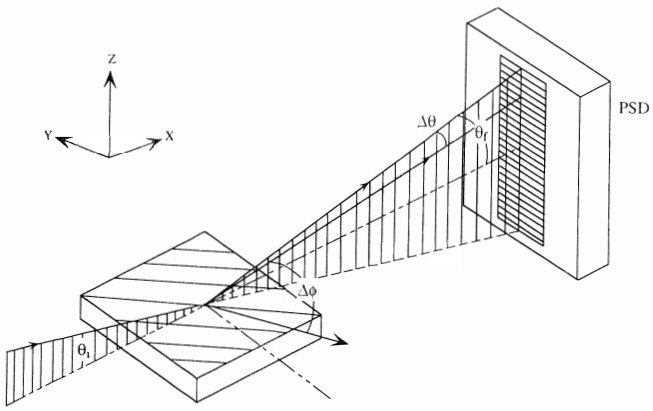

FIG. 1. Geometry of forward and lateral scattering of neutrons sent at grazing incidence to the surface.

Beautiful and delicate work has been done (mostly by x rays) to study phenomena[4–6] characterized by a finite value of τ_y. Here the scattering data were analyzed in terms of the first Born approximation.[7,8] Groundbreaking observations have been made in the forward-scattering geometry. The scattering from rough surfaces has been analyzed in the framework of the distorted wave Born approximation.[9,10] Conformal propagation of roughness in multilayers has been monitored in selected metallic and semiconducting systems. The procedure used consisted in calculating the forward scattering for a

mean depth density profile plus some model lateral dishomogeneity. Often good agreement with the data was found;[5,11–14] however, the models proposed never stemmed directly from the scattering data. The purpose of this paper is to show the forward scattering of two types of polymer multilayers having large roughness, with nanometer high lateral perturbations. It will be seen that the scattering figures are well structured, showing ridges of maxima that can be indexed in terms of scattering modes. The data show features that might aid in the interpretation of the scattering.

The first example shows the forward scattering from a film made of a symmetric, diblock copolymer or polystyrene (PS) and polymethylmethacrylate (PMMA), denoted P(S-b-MMA). The molecular weight of each block is $\sim 5\times 10^4$. Thin films of P(S-b-MMA), cast onto silicon substrates, heated to temperatures above the glass transition temperature ($\sim 100\,^\circ$C), microphase separate into a multilayered, lamellar morphology.[15] The lamellae are oriented parallel to the film surface, and at any point in the specimen the thickness is given by $(n+1/2)L$ where n is an integer and L is the periodicity of the layers (for this copolymer $L=520$ Å). PMMA segregates to the substrate and PS to the air surface. Films with a total thickness not commensurate with the layer thickness form islands or holes at the surface.[16] The multilayered configuration of the copolymer is made more visible to neutrons by substituting the hydrogen with deuterium in the PS block of the copolymer (the neutron-scattering length density of polystyrene is 1.5×10^{-6} Å^{-2}, while that of deuterated PS is 6.5×10^{-6} Å^{-2}). The sample studied here had a thickness of 3.4×10^3 Å which corresponds to $n=6$ layers and was annealed at 190 °C for 240 h to achieve equilibrium. Disorder was introduced into the layered structure by the addition of 10% of pure PMMA homopolymer ($M_W=5\times 10^4$) to the copolymer.

Neutron-scattering measurements were performed on the POSY II reflectometer[17] at the Intense Pulsed Neutron Source at Argonne National Laboratory. In this instrument a pulsed beam of neutrons, of all wavelengths in the thermal range, are brought on the sample at an angle θ_i. A position sensitive detector records the specularly reflected neutrons at $\theta_f=\theta_i$ as well as the scattered neutrons at $\theta_f\neq\theta_i$ as a function of the time-of-flight, and thus of their wavelength. The detector is position sensitive only in the θ_i,θ_f plane with a resolution of $\Delta\theta\sim 0.02°$, whereas for lateral scattering the resolution is relaxed ($\Delta\phi=0.2°$). In practice the measurements integrate over τ_y.

Figure 2 shows the contour plot of the intensities obtained for P(S-b-MMA) at $\theta_i=1.58°$. The abscissa is given in terms of the angle of scattering from the incident beam $\theta_i+\theta_f$ and the ordinate as the neutron wavelength. Well visible is the specular reflectivity at $\theta_i=\theta_f$. The angle $\theta_f=0$ corresponds to the surface horizon, which divides the neutrons scattered back in free space from those refracted into the substrate and exciting from its edge. As in a Laue camera, here the whole scattering spectrum is recorded. However, the spectrum is also too rich to be easily interpretable. To simplify the presentation only the positions of the local maxima are plotted in Fig. 3. The combined datasets for the runs at $\theta_i=0.6°$, $1.05°$, and $1.58°$ form a simple pattern that can be interpreted in terms of the salient characteristics of the specular reflectivity.

The specular reflectivity is obtained by taking a strip of intensity at $\theta_i=\theta_f$, of width equal to the instrumental resolution and normalizing it to the incident wavelength spectrum. The inset in Fig. 3 shows the reflectivity R multiplied by q_z^4 as a function of $q_z=k_{zi}+k_{zf}$, since Rq_z^4

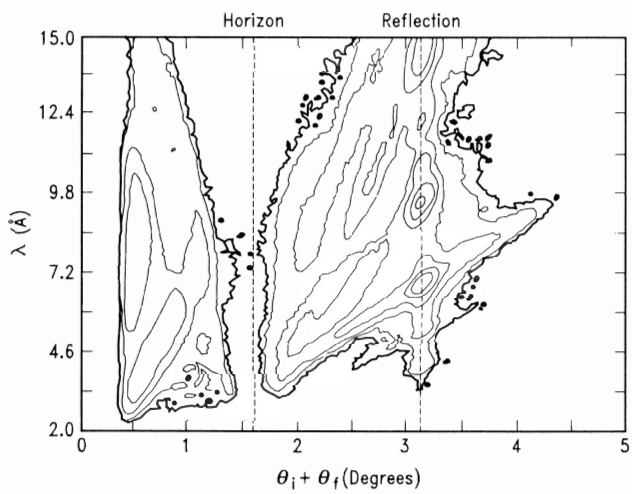

FIG. 2. Contour plot (log scale) of the forward scattering from a multilayer of PS-PMMA copolymers with 10% PMMA added. Angle of incidence: $\theta_i=1.58°$. In the abscissa θ_f is the exiting angle. $\theta_f=0$ is the horizon of the sample surface and the limit for neutrons reemitted form the surface. The specularly reflected beam is at $\theta_i=\theta_f$.

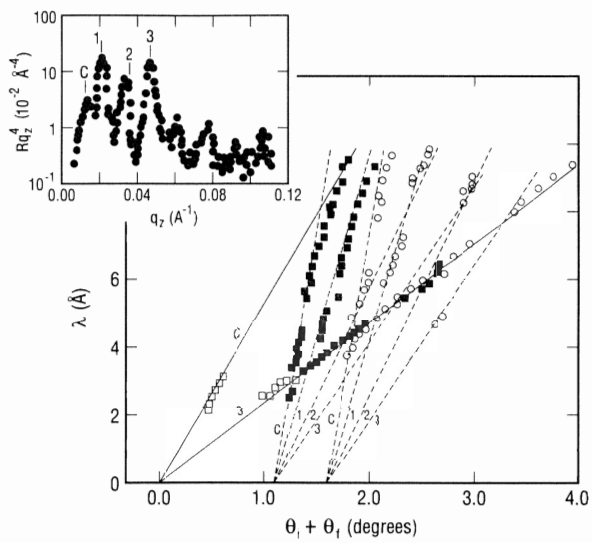

FIG. 3. Scattering maxima for the sample of Fig. 2, for three different angles of incidence. Open squares: $\theta_i=0.6°$, full squares: $\theta_i=1.05°$; open circles: $\theta_i=1.58°$. Most of the maxima relative to the specular reflection have been omitted. Dashed lines represent Eq. (2) in the form: $(\theta_i+\theta_f)(1/q_{zM})-\theta_i(1/q_{zM})=\lambda/4\pi$; Full lines represent Eq. (3), which here becomes $(\theta_i+\theta_f)\cdot 2\pi/q_{zM}=\lambda$; In the inset: specular reflectivity of the same sample.

tends to a constant value for large values of q_z. Peaks are visible at the critical momentum ($q_{zc}=0.012$ Å^{-1}) and at the strong interference maxima at $q_{z1}=0.0208$, $q_{z2}=0.0336$, and $q_{z3}=0.0468$ Å^{-1} (the difference between adjacent maxima, $\Delta q_z \sim 2\pi/L$, where L is the periodicity of the layer). Outside of the specular reflection, scattering appears at

$$2\pi \sin\theta_f/\lambda = q_{zM}/2 = k_{zM} \tag{2}$$

with q_z taking one of the value listed above. Equation (2), is presented in Fig. 3 in the form of dashed lines. Clearly these describe the positions of the majority of datapoints. The location of the ridges is independent of the angle of incidence θ_i: in Eq. (2) appear only some special values of the momenta of the remitted neutrons. The constant-k_z scattering at the critical angle was discovered by Yoneda a long time ago.[18] At least one observation[5] has been made recently of constant-k_z scattering of other interference maxima of the reflectivity. Qualitatively the mechanism that gives rise to the diffuse scattering may be described in the following way. The lateral imperfections scatter the incident plane wave into spherical waves. These may be thought as composed of plane waves which, for special values q_{zM}, are reflected by the laterally averaged sample. In this pictorial description scattering at k_{zM} occurs as a sequence of two events, first the incoherent scattering from the lateral imperfections, second the coherent scattering from the mean lattice.

Some of the data points do not fit along the traced lines, but instead are aligned along a straight line common to all scattering spectra regardless of the angle of incidence. The strongest of these is identified as

$$k_{zi} + k_{zf} = q_{z3} \ . \tag{3}$$

The constant-q_z scattering has also been observed before. Often it has been attributed to "conformal roughness," which means that subsequent interfaces are in registry but only over limited areas.[5,11–13] The term covers a wide range of situations: the film may be conformal from top to bottom, or only in part; the lateral mismatch in the layering may be due to orientational misalignment or to unequal growth. The synthetic display of Fig. 3 shows that constant$=k_z$ and constant-q_z types of ridges are coexisting in the scattering from one sample. At their intersection different ridges do not follow an exact linear relation, i.e., are not at constant q_z or constant k_z. Instead, the phenomenology is akin to that displayed in the diffraction from perfect crystals when two Bragg reflections are simultaneously excited. Finally, notice that only one constant-q_z line obeying Eq. (3) is clearly visible for this film.

The second sample to be tested consists of a diblock copolymer of poly(ethylene-propylene)-polyethylethylene (PEP-PEE), of molecular weight 5.7×10^4 with 55% PEP by volume.[19] For neutron contrast the hydrogen of the propylene was substituted with deuterium. PEP-PEE undergoes an order-disorder transition at 125° C. Below that temperature, the material has lamellar structure with a 340-Å period which, in a well annealed thin film, is parallel to the surface. For this copolymer PEE segregates to both the air and the substrate interfaces and, consequently, the thickness at any point is given by nL. Since in our sample the initial thickness, approximately 3000 Å, was not a multiple of L, the last layer was not complete. When examined with a microscope, the surface did not appear entirely flat, but exhibited wells with depth estimated to be equal to L. These were the only recognizable defects in this multilayered structure.

In Fig. 4 are plotted the positions of the maxima of the forward scattering of the PEP-PEE sample for angles of incidence $\theta_i=0.33°$, 1.01°, and 1.67°. Regardless of the angle of incidence the data fall on straight lines that extrapolate to the origin. Following the procedure developed above, Rq_z^4 is plotted as a function of q_z: the leading reflectivity maxima occur at $q_{zc}=0.0096$, $q_{z1}=0.0222$, $q_{z2}=0.0420$, $q_{z3}=0.0570$ Å^{-1}. Substituting into Eq. (3), these values yield the solid lines in Fig. 4. Here virtually all the reflectivity maxima give rise to constant q_z ridges, while the constant-k_z scattering is not visible— not even for the critical edge. However, some of the datapoints of Fig. 4 do not fall on constant q_z. Precisely, for $q_z=q_{z1}$, bifurcations appear for the data taken at angles of incidence $\theta_i=1.01°$ and 1.67°. Visual inspection shows that the bifurcations take place when the exit beam is equal to the critical edge: $k_f=k_c$. Below this angle the new branches represent a sequence of two scattering processes:

$$k_{zi} + k_{zv} = q_{z1}; \quad k_{zv} + k_{zf} = q_{zc} \ . \tag{4}$$

Here k_{zv} represents a virtual, intermediate scattering vector; the incident and the exit momenta are still k_{zi} and k_{zf}. The new loci are drawn as dashed-dotted lines in Fig. 4. The scattering from the PEP-PEE sample does not show evidence of constant-k_z scattering, but on top of the simple constant-q_z modes there are modes where two q_z are coupled.

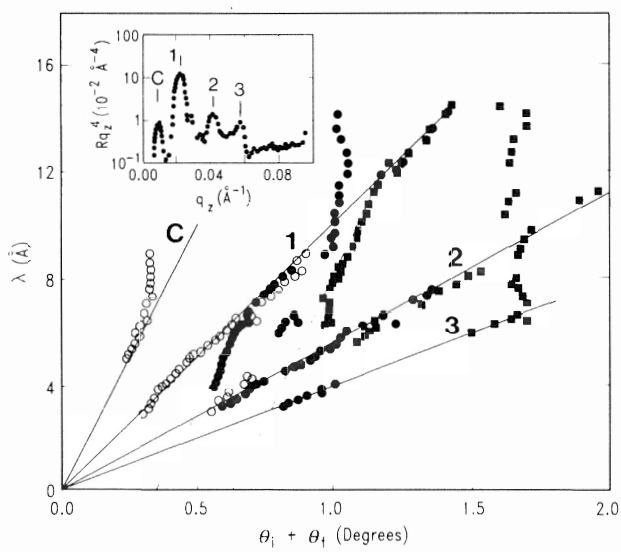

FIG. 4. Scattering maxima for an annealed PEP-PEE diblock copolymer sample, three angles of incidence. Open circles: $\theta_i=0.33°$; full circles: $\theta_i=1.01°$; full squares: $\theta_i=1.67°$. The dot-point lines are discussed in the text. In the inset, the specular reflectivity of the same sample.

The forward scattering of imperfect multilayers can be quite structured, as was illustrated with two examples (not necessarily inclusive) drawn from the study of partially deuterated copolymers. The scattering of a "white" neutron beam obtained from a pulsed neutron source provides most naturally a complete scan of a portion of the scattering space, although the resolution is often less than desirable and the range of the **q** space spanned is limited. The topology of the maxima of the scattered neutrons can be described in terms of constant-k_z and constant-q_z lines. At their intersection the lines are not entirely straight, indicating the presence of coupling between different scattering modes. In the dynamical theory of scattering (or for that matter in the Rayleigh scattering from surfaces) simultaneously diffracted beams show at their intersection a coupling which is described by a rather simple expression, which contains only the Fourier components of the scattering potential relative to the intervening modes. If, in a similar spirit, a scheme were devised for forward scattering, much more direct information would be obtained on the nature of disorder at the surface and below in the growing number of systems displaying a thin layered structure.

One of us (G.P.F.) would like to thank S. K. Sinha for many enlightening discussions. Work at Argonne was supported by the U.S. Department of Energy, Basic Energy Sciences, under Contract No. W-31-109-ENG-38.

---

*Present address: Foundation for Research and Technology-Hellas, Heraklion, Crete, Greece.

†Present address: Department of Polymer Science, University of Akron, Akron, OH 44325-3801.

[1]O. Glatter and O. Kratky, *Small Angle X-Rays Scattering,* (Academic, London, 1982).

[2]J. Cotton, in *Neutron, X-Ray and Light Scattering,* edited by P. Lindner and Th. Zemb (North-Holland, Amsterdam, 1991).

[3]T. P. Russell, Mater. Sci. Rep. **5**, 171 (1990).

[4]J. Penfold and R. K. Thomas, J. Phys. C **2**, 1369 (1990).

[5]S. K. Sinha, Physica B **173**, 25 (1991).

[6]M. Tolan, G. König, L. Brügemann, W. Press, F. B. Brinkop, and J. P. Kotthaus, Europhys. Lett. **20**, 223 (1992).

[7]I. K. Robinson and E. Vlieg, in *Surface X-ray and Neutron Scattering,* edited by H. Zabel and I. K. Robinson, Springer Proceedings in Physics, Vol. 61 (Springer-Verlag, Berlin, 1992), p. 51.

[8]J. Als Nielsen and K. Kjaen, in *Phase Transitions in Soft Condensed Matter,* edited by T. Riste and D. Sherrington (Plenum, New York, 1988).

[9]S. K. Sinha, E. B. Sirota, S. Garoff, and H. B. Stanley, Phys. Rev. B **38**, 2297 (1988).

[10]R. Pynn, Phys. Rev. B **45**, 602 (1992).

[11]D. G. Stearns, J. Appl. Phys. **71**, 4286 (1992).

[12]Y. H. Phang, D. E. Savage, R. Kariotis, and M. G. Lagally, J. Appl. Phys. **74**, 3181 (1993).

[13]D. Bahr, W. Press, R. Jebasinski, and S. Mantl, Phys. Rev. B **47**, 4385 (1993).

[14]J. B. Kortright, J. Appl. Phys. **70**, 3620 (1991).

[15]S. H. Anastasiadis, T. P. Russell, S. K. Satija, and C. F. Majkrzak, Phys. Rev. Lett. **62**, 1852 (1989); J. Chem. Phys. **92**, 5677 (1990).

[16]G. Coulon, T. P. Russell, V. R. Deline, and P. F. Green, Macromolecules **22**, 2581 (1989).

[17]A. Karim, B. H. Arendt, R. Goyette, Y. Y. Huang, R. Kleb, and G. P. Felcher, Physica B **173**, 17 (1991).

[18]Y. Yoneda, Phys. Rev. **131**, 2010 (1963).

[19]F. S. Bates, J. H. Rosedale, and G. H. Fredrickson, J. Chem. Phys. **92**, 6255 (1990).